



Synthesis and properties of triphenylamine-based hydrazones with reactive vinyl groups

V. Mimaite^a, J.V. Grazulevicius^{a,*}, J. Ostrauskaite^a, V. Jankauskas^b

^a Department of Organic Technology, Kaunas University of Technology, Radvilenu pl. 19, LT-50254 Kaunas, Lithuania

^b Department of Solid State Electronics, Vilnius University, Sauletekio Aleja 9, LT-2040, Vilnius, Lithuania

ARTICLE INFO

Article history:

Received 5 December 2011

Received in revised form

6 March 2012

Accepted 11 March 2012

Available online 29 March 2012

Keywords:

Hydrazone

Triphenylamine

Vinyl group

Polymerization

Charge mobility

Methoxy group

ABSTRACT

Two triphenylamine-based hydrazones with reactive vinyl groups were synthesized and characterized. The optical, thermal, electrochemical and photoelectrical properties of the obtained compounds were studied. All the synthesized hydrazone monomers form glasses with the glass transition temperatures ranging from 52 °C to 82 °C. The electron photoemission spectra of the synthesized hydrazones were recorded and ionization potentials of 5.22–5.29 eV were established. Room temperature hole-drift mobilities in the amorphous film of hydrazone monomer having three vinyl groups established by xerographic time-of-flight technique was found to be $3.5 \times 10^{-3} \text{ cm}^2/\text{V}\cdot\text{s}$ at an electric field of $6.4 \times 10^5 \text{ V}\cdot\text{s}$. Self-polymerization of the hydrazones bearing vinyl groups was demonstrated by differential scanning calorimetry. Self-polymerization of monomers containing one and three vinyl groups started at 151 °C and 136 °C, while maximum polymerization rates were observed at 209 °C and 167 °C respectively.

© 2012 Elsevier Ltd. All rights reserved.

1. Introduction

Organic semiconductors are currently widely used in different optoelectronic and electronic devices [1–5]. Aromatic hydrazones are among the most effective organic hole-transporting materials [6]. Due to relatively high hole-drift mobilities, the simplicity of synthesis, good compatibility with inert polymer hosts hydrazones are widely used in electrophotographic photoreceptors of copying machines, laser printers, fax machines [7]. They also showed promising performance as hole-transporting glass-forming materials in dye sensitized solar cells [8,9], as unimolecular half-substrators for molecular processors [10], and as active media in memory devices [11]. It is known efficient organic optoelectronic devices can be obtained most often by building multilayer structures [12]. The main difficulty in the preparation of such devices by solution processing is the solubility of the material which forms the bottom layer onto which the top layer has to be cast, because most organic semiconductors are soluble in the same solvents. One approach that was employed to circumvent this problem is the appliance of electroactive derivatives with reactive functional groups, which could be converted into insoluble networks by cross-linking reactions. Several series of electroactive materials with

reactive functional groups, including hydrazones were described [13–18]. Most of the polymerizable hydrazones reported until now contained reactive epoxy groups. They could be converted into polymers either by polyaddition or cationic polymerization. In this work we report on the synthesis of triphenylamine-based hydrazones with reactive vinyl groups and demonstrate the possibility of their self-polymerization.

2. Experimental

2.1. Instrumentation

¹H NMR spectra were taken on a Varian Unity Inova (300 Hz) spectrometer. IR spectra were recorded with Perkin Elmer Spectrum GX II FT-IR System. Mass spectra were obtained on a Waters ZQ 2000 mass spectrometer. UV and fluorescence (FL) spectra of 10^{-4} M solutions of the synthesized compounds were recorded in quartz cells using a Perkin Elmer Lambda 35 spectrometer and Hitachi MPF-4 spectrofluorophotometer respectively. Thermogravimetric analysis (TGA) was performed on Mettler TGA/SDTA851e/LF/1100 apparatus at a heating rate of 20 °C/min under nitrogen atmosphere. Differential scanning calorimetry (DSC) measurements were performed on DSC Q 100 TA Instrument at a heating rate of 10 °C/min under nitrogen atmosphere. Cyclic voltammetry (CV) measurements were carried out with a glassy carbon working

* Corresponding author. Tel.: +370 37 300193; fax: +370 37 300152.

E-mail address: juozas.grazulevicius@ktu.lt (J.V. Grazulevicius).

electrode in a three electrode cell. The measurements were carried out in dry dichloromethane solution containing 0.1 M tetrabutylammonium perchlorate as electrolyte at room temperature under nitrogen atmosphere. Each measurement was calibrated with the standard ferrocene/ferrocenium (Fc/Fc⁺). The ionization potentials (I_p) of the films of the synthesized compounds measured by the electron photoemission in air method as described previously [19]. The measurement method was, in principle, similar to that demonstrated by Miyamoto et al. [20]. The samples for the ionization potential measurements were prepared by dissolving compounds in tetrahydrofuran and casting thin layers on Al plates, pre-coated with ca. 0.5 μm thick adhesive layer of the copolymer of methylmethacrylate and methacrylic acid (MKM). The function of this layer was not only to improve adhesion but also to eliminate electron photoemission from Al. No photoemission was detected from Al plate overcoated with MKM at illumination with up to 6.25 eV quanta energy light. In addition, the MKM layer is conductive enough to avoid charge accumulation on it during measurements. The samples were illuminated with monochromatic light from the quartz monochromator with deuterium lamp. The power of the incident light beam was $(2\text{--}5) \times 10^{-8}$ W. The negative voltage of 300 V was supplied to the sample substrate. The counter-electrode with the 4.5 mm \times 15 mm slit for illumination was placed at 8 mm distance from the sample surface. The counter-electrode was connected to the input of the BK2-16 type electrometer, working in the open impute regime, for the photocurrent measurement. The strong photocurrent of $10^{-15}\text{--}10^{-12}$ A was flowing in the circuit under illumination. Hole-drift mobility measurements were performed by a xerographic time-of-flight (XTOF) method [21]. The samples for the charge mobility measurements were prepared as described earlier [22].

2.2. Materials

The starting compounds aniline (Aldrich), 4-iodanisole (Aldrich), triphenylamine (Aldrich), phenylhydrazine (Fluka), 1-(chloromethyl)-4-vinylbenzene (Aldrich), and the required chemicals, i.e. copper powder (Aldrich), 18-crown-6 (Aldrich), phosphorous (V)

oxychloride (Aldrich), tetrabutylammonium hydrogensulfate (Aldrich), sodium acetate (Aldrich), potassium carbonate (Lachner), anhydrous sodium sulfate (Penta), potassium hydroxide (Aldrich), were purchased as reagent grade chemicals and used as received. 4-Methoxy-*N*-(4-methoxyphenyl)-*N*-phenylamine (**1**) was synthesized by Ullmann coupling reaction according to the procedures outlined in the literature [23]. 4-(Bis(4-methoxyphenyl)amino)benzaldehyde (**2**) and tris(4-formylphenyl)amine (**3**) were synthesized by the method of Vilsmeier as described in the literature [23,24].

2.2.1. 4-(Bis(4-methoxyphenyl)amino)benzaldehyde *N*-phenylhydrazone (**4**)

Phenylhydrazine (1 ml, 10.4 mmol) was added to the solution of aldehyde (**2**) (1.7 g, 5.2 mmol) in 10 ml of methanol. The reaction mixture was refluxed at 65 °C with stirring for ca. 0.5 h until no aldehyde was left (TLC monitoring). After cooling, yellowish precipitate was filtered, washed with large amount of methanol and dried.

The yield of **4** was 1.9 g (85%).

IR (KBr), ν/cm^{-1} : 3319 (N–H), 3027, 3000 (ar. C–H), 2956, 2932, 2908 (alif. C–H), 2837 (O–CH₃), 1599, 1505 (ar. C=C), 1296 (C–N), 1241 (C–O–C).

¹H NMR (CDCl₃), δ (ppm): 3.84 (s, 6H, OCH₃), 3.85 (s, 1H, NH), 6.88 (d, 5H, $J = 9$ Hz, Ar), 6.94 (d, 2H, $J = 9$ Hz, Ar), 7.11 (d, 5H, $J = 9.3$ Hz, Ar), 7.17 (d, 1H, $J = 9$ Hz, Ar), 7.29 (t, 2H, $J = 7.8$ Hz, Ar), 7.49 (d, 2H, $J = 8.4$ Hz, Ar), 7.67 (s, 1H, $J = 8.7$ Hz, CH).

MS (APCI⁺, 20 V), m/z (%) = 501 [M + H]⁺, 423, 332.

2.2.2. Tris(4-formylphenyl)amine tri(*N*-phenylhydrazone) (**5**)

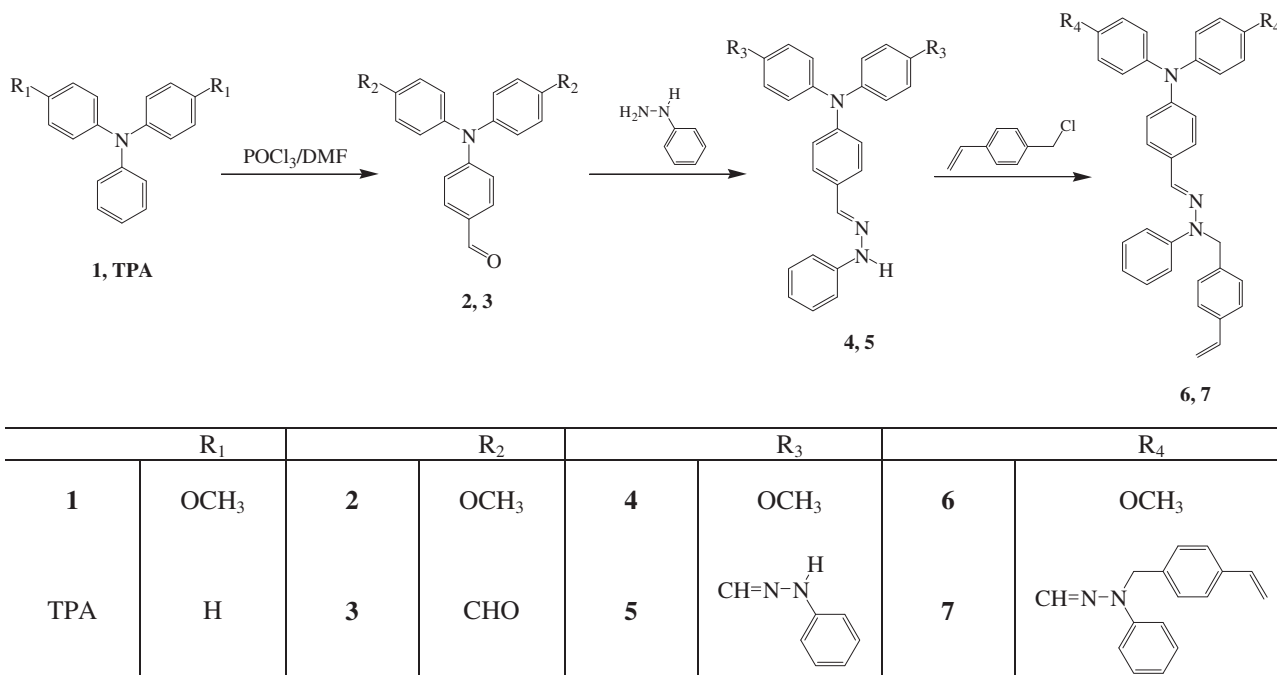
Compound **5** was synthesized from phenylhydrazine (1 ml, 10.4 mmol) and trialdehyde **3** (0.5 g, 1.7 mmol) by the same procedure as compound **4**.

The yield of **5** was 0.9 g (88%).

IR (KBr), ν/cm^{-1} : 3309 (N–H), 3028 (ar. C–H), 2959 (alif. C–H), 1596, 1497, 1446 (ar. C=C), 1321 (C–N), 1259 (C–O–C).

¹H NMR (CDCl₃), δ (ppm): 3.84 (s, 3H, NH), 6.69–6.72 (m, 6H, Ar), 6.76 (t, 3H, $J = 8.2$ Hz, Ar), 6.85–6.89 (m, 6H, Ar), 6.95–7.01 (m, 9H, Ar, CH), 7.03–7.06 (m, 6H, Ar).

MS (APCI⁺, 20 V), m/z (%) = 600 [M + H]⁺, 510, 313, 245.



Scheme 1. Synthetic routes compounds **6** and **7**.

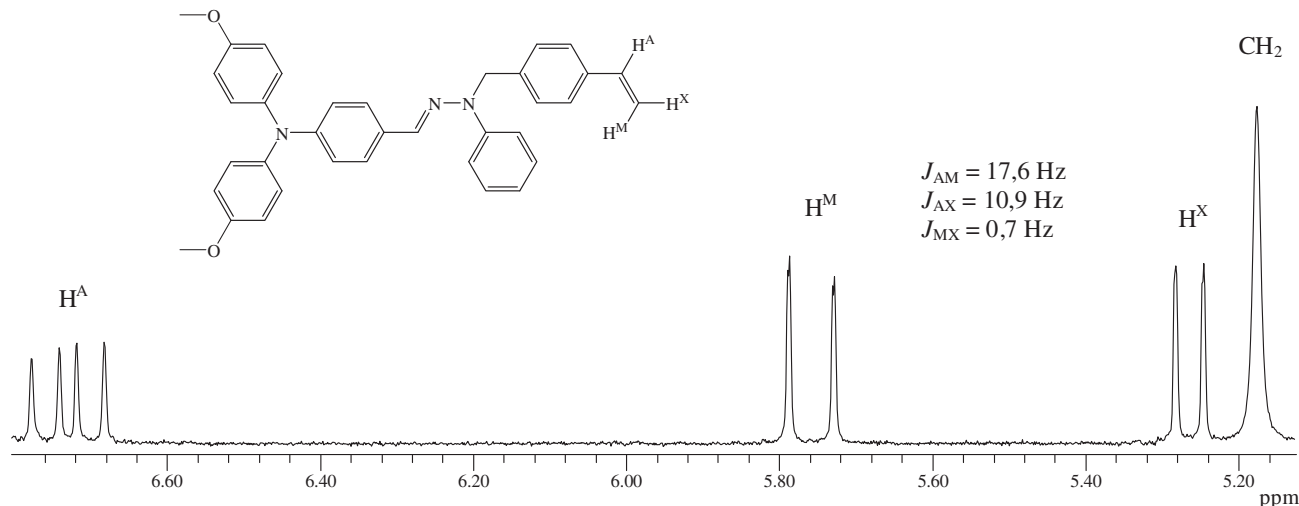


Fig. 1. Fragment of ^1H NMR spectrum of hydrazone monomer **6** in CDCl_3 .

2.2.3. 4-(Bis(4-methoxyphenyl)amino)benzaldehyde *N*-4-vinylbenzyl-*N*-phenylhydrazone (**6**)

Hydrazone (**4**) (1 g, 2.4 mmol) was dissolved in 5 ml of acetone and 1-(chloromethyl)-4-vinylbenzene (0.7 ml, 4.8 mmol) was added drop-wise. The reaction mixture was heated to the reflux temperature and tetrabutylammonium hydrogensulfate (0.008 g, 0.024 mmol) as well as KOH (0.81 g, 19.5 mmol) were added to the reaction mixture. The later was added in three portions with 5 min interval. After 30 min inorganic components were filtered off and the solvent was removed by distillation. The product was purified by column chromatography at the reduced pressure. The mixture of ethyl acetate and hexane in a volume ratio of 1:5 was used as an eluent. The resin-like crude product was dissolved in diethyl ether and precipitated into the methanol. It was recrystallized from methanol.

The yield of **6** was 0.6 g (46%), mp. 64–66 °C.

IR (KBr), ν/cm^{-1} : 3039 (ar. C–H), 2970, 2933 (alif. C–H), 2836 (O–CH₃), 1585, 1516, 1484 (ar. C=C), 1387 (C=N–N), 1338 (C–N), 1258 (C–O–C), 1630, 992, 910 (CH=CH₂).

^1H NMR (CDCl_3), δ (ppm): 3.79 (s, 6H, OCH₃), 5.13 (s, 2H, CH₂), 5.22 (dd, 1H AMX of system CH=CH₂ proton H^X cis $J_{AX} = 10.9$ Hz),

5.72 (dd, 1H AMX of system CH=CH₂ proton H^M trans $J_{AM} = 17.6$ Hz ir gem $J_{MX} = 0.7$ Hz), 6.69 (dd, 1H AMX of system CH=CH₂ proton H^A), 6.81 (d, 4H, $J = 9.1$ Hz, Ar), 6.86–6.93 (m, 3H, Ar), 7.04 (d, 4H, $J = 8.7$ Hz, Ar), 7.18 (d, 2H, $J = 8.1$ Hz, Ar), 7.27 (d, 2H, $J = 9.9$ Hz, Ar), 7.31–7.38 (m, 5H, Ar, C–H), 7.43 (d, 2H, $J = 8.8$ Hz, Ar).

MS (APCI⁺, 20 V), m/z (%) = 540 [M + H]⁺, 539, 423, 332.

2.2.4. Tris(4-formylphenyl)amine tri(*N*-4-vinylbenzyl-*N*-phenylhydrazone) (**7**)

Compound **7** was synthesized by the same procedure as compound **6** using hydrazone **5** (0.8 g, 1.3 mmol), 1-(chloromethyl)-4-vinylbenzene (1.1 ml, 7.9 mmol), tetrabutylammonium hydrogensulfate (0.004 g, 0.013 mmol) and KOH (1.3 g, 23.4 mmol). The target compound was purified by column chromatography at the reduced pressure using ethyl acetate and hexane in a volume ratio of 1:9 as an eluent.

The yield of **7** was 0.5 g (42%).

IR (KBr), ν/cm^{-1} : 3036, 3005 (ar. C–H), 1596, 1508, 1496 (ar. C=C), 1394 (C=N–N), 1318 (C–N), 1628, 990, 908 (CH=CH₂).

^1H NMR (CDCl_3), δ (ppm): 5.15 (s, 6H, CH₂), 5.23 (dd, 1H of system AMX CH=CH₂ proton H^X cis $J_{AX} = 10.9$ Hz), 5.71 (dd, 1H of system AMX CH=CH₂ proton H^M trans $J_{AM} = 17.6$ Hz ir gem $J_{MX} = 0.7$ Hz), 6.69 (dd, 1H of system AMX CH=CH₂ proton H^A), 6.93 (t, 3H, $J = 7.2$ Hz, Ar), 7.03 (d, 6H, $J = 8.8$ Hz, Ar), 7.19 (d, 6H, $J = 8.1$ Hz, Ar), 7.27–7.39 (m, 21H, CH, Ar), 7.49 (d, 6H, $J = 8.4$ Hz, Ar).

MS (APCI⁺, 20 V), m/z (%) = 949 [M + H]⁺, 948, 832, 740, 327.

3. Results and discussion

The synthetic routes to hydrazones with reactive vinyl groups (**6**, **7**) are shown in Scheme 1. The first step was Ullmann coupling reaction to get triphenylamine derivative **1** with methoxy groups at *para* position. The second step was formylation of compounds **1** and triphenylamine (TPA) by the method of Vilsmeier. The next step was the condensation of aldehydes **2**, **3** with phenylhydrazine. In

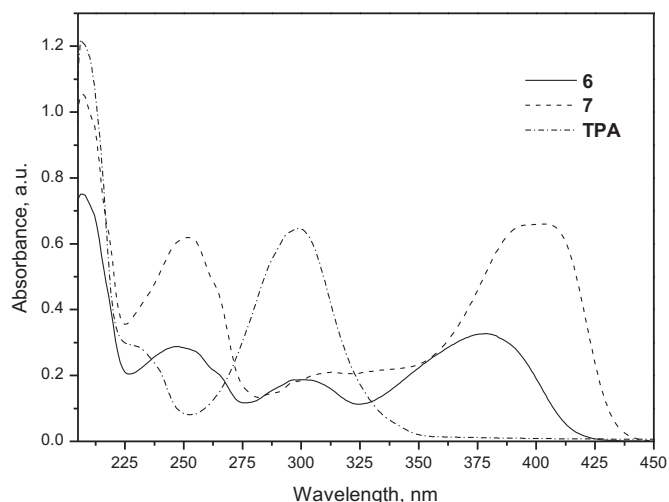


Fig. 2. UV spectra of dilute THF solutions of monomers **6**, **7** and TPA.

Table 1
The optical characteristics of **6**, **7** and TPA.

| Compound | UV, λ_{max} (nm) | PL, λ_{max} (nm) |
|----------|---------------------------------|---------------------------------|
| 6 | 206, 248, 298, 378 | 448 |
| 7 | 206, 252, 303, 401 | 448 |
| TPA | 206, 236, 299 | |

Table 2
Thermal characteristics of **6** and **7**.

| Compound | $T_{\text{deg-5\%}}$ ($^{\circ}\text{C}$) | T_m^a ($^{\circ}\text{C}$) | T_g^b ($^{\circ}\text{C}$) |
|----------|---|--------------------------------|--------------------------------|
| 6 | 307 | 65 | 52 |
| 7 | 315 | – | 82 |

^a First heating scan.

^b Second heating scan.

the last step monomers **6** and **7** were obtained by interaction of compounds **4**, **5** with 1-(chloromethyl)-4-vinylbenzene. All the reactions were controlled by TLC. The synthesized compounds were purified by column chromatography and characterized by IR-, ^1H NMR- and mass spectrometries.

The proton signals of methoxy groups at 3.79 ppm are present in the ^1H NMR spectrum of compound **6**. The characteristic signals of vinyl groups are observed in the ^1H NMR spectra of the hydrazone monomers (**6**, **7**). Three protons of vinyl group form three-spin AMX system (Fig. 1). According to the coupling constants protons are assigned to the corresponding signals. The signals of H^A protons, which are near benzene ring, are observed at 6.69 ppm. The signals of H^X and H^M protons are observed at 5.22–5.23 ppm and 5.71–5.72 ppm respectively. The signals of CH_2 group protons of the hydrazone moiety of compounds **6** and **7** are observed at 5.13 and 5.15 ppm respectively.

Absorption bands of NH group observed in the IR spectra of hydrazones **4**, **5** at $3309\text{--}3319\text{ cm}^{-1}$ disappear in the spectra of monomers **6**, **7**. The characteristic stretches of vinyl groups appear in the IR spectra of hydrazones **6**, **7** at $1628\text{--}1630\text{ cm}^{-1}$, $990\text{--}992\text{ cm}^{-1}$ and $910\text{--}908\text{ cm}^{-1}$.

Mass spectra of all the synthesized compounds show the corresponding molecular ion peaks.

UV spectra of dilute solutions of compounds **6**, **7** and that of TPA in THF are given in Fig. 2. The wavelengths of absorption maxima are summarized in Table 1.

Absorption of hydrazones **6**, **7** is red shifted with respect to that of TPA. This shift can be attributed to $\pi \rightarrow \pi^*$ transitions and is the consequence of increased conjugated π -electron system due to the incorporation of hydrazone moieties into the structure of TPA. The lowest energy absorption band of compound **7** having three hydrazone moieties is red shifted with respect of that of compound **6** containing one hydrazone moiety.

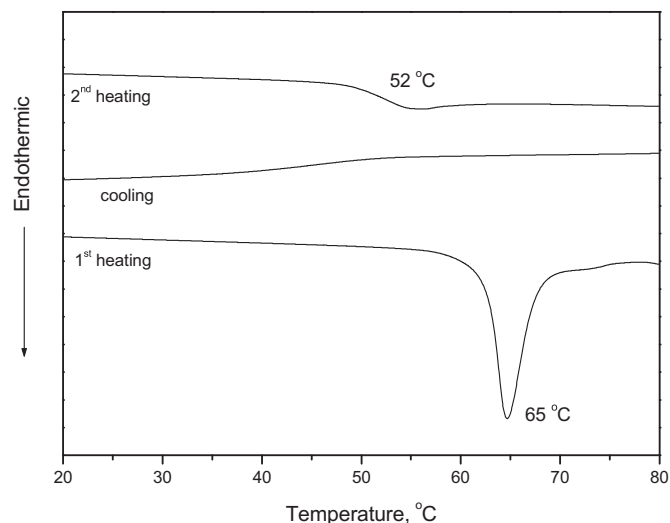


Fig. 4. DSC curves of **6** at the heating/cooling rate of $10\text{ }^{\circ}\text{C}/\text{min}$ in N_2 atmosphere.

Compounds **6**, **7** exhibit blue fluorescence when excited with UV irradiation. Their fluorescence maxima appear at 448 nm.

The thermal properties of hydrazones **6**, **7** were studied by DSC and TGA. The temperatures of thermal transitions are summarized in Table 2.

Compounds **6**, **7** demonstrate relatively high thermal stability. Their 5% weight loss temperatures are $307\text{ }^{\circ}\text{C}$ – $315\text{ }^{\circ}\text{C}$ respectively. These are rather high stabilities as for aromatic hydrazones. Earlier reported 5% weight loss temperatures for carbazole-based hydrazones ranged from $260\text{ }^{\circ}\text{C}$ to $290\text{ }^{\circ}\text{C}$ [25]. Thermogravimetric curves of compounds **6**, **7** is shown in Fig. 3. The thermal degradation of both hydrazones (**6** and **7**) occurs in two stages however the mechanism of the process is clearly dependent on the number of hydrazone moieties in the molecule. The rate of the thermal decomposition of compound **7** containing three hydrazone moieties is considerably slower than that of compound **6** having one hydrazone moiety.

DSC investigations revealed that hydrazone monomer **6** could exist both in crystalline and amorphous states while compound **7**

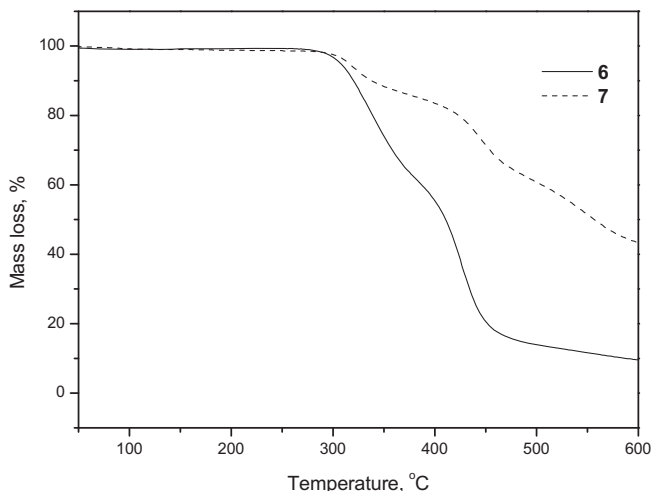


Fig. 3. TGA curves of monomers **6**, **7** at the heating rate of $20\text{ }^{\circ}\text{C}/\text{min}$ in N_2 atmosphere.

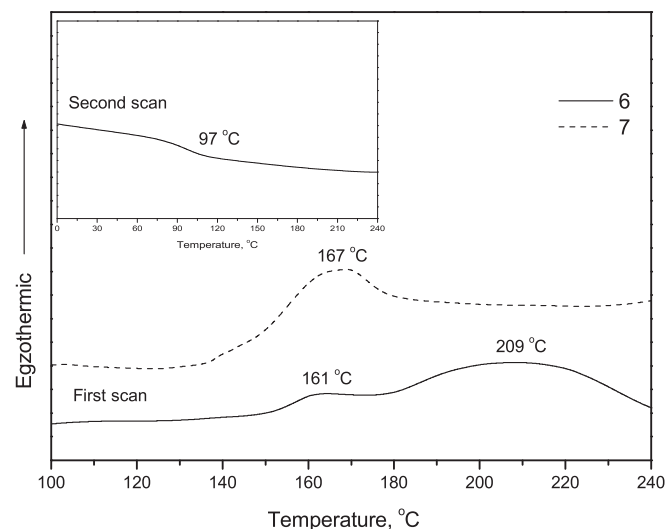


Fig. 5. DSC curves of **6** and **7** at the heating/cooling rate of $10\text{ }^{\circ}\text{C}/\text{min}$ in N_2 atmosphere.

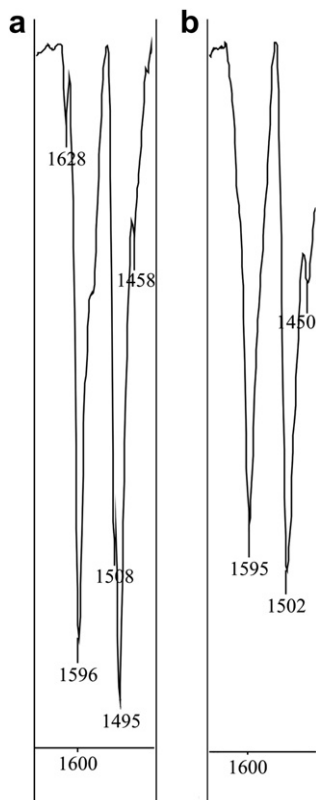


Fig. 6. Fragments of IR spectra of hydrazone monomer **7** (a) and of the product of its self-polymerization (b).

was found to be amorphous. The DSC thermogram of hydrazone **6** is presented in Fig. 4. The first DSC heating scan of **6** showed endothermic melting signal 65 °C. No signal of crystallization was observed in the cooling scan and the following heating scan revealed only a glass transition at 52 °C.

Compound **7** exhibited only glass transition in the first and the following DSC scans. Hydrazone **7** having three hydrazone moieties showed by 30 °C higher glass transition temperature than compound **6** with one hydrazone substituent. This observation can apparently be explained by the higher molecular weight of compound **7** which results in stronger intermolecular interaction.

Self-polymerization of the monomers **6** and **7** was studied by DSC. The results are presented in Fig. 5. During the heating scan of **6** two exothermic peaks were observed with maxima at 161 °C and 209 °C. It can be assumed that the first peak is due to the step of thermal-initiation and the second one is due to the propagation [26]. These results are comparable with the earlier reported observation. Huang et al. [27] observed self-polymerization of aromatic amine with two vinyl groups in the range of 150–180 °C. The glass transition temperature of the product of polymerization of **6** was found to be 97 °C which is considerably higher than that of the monomer (**6**) itself (52 °C). Self-polymerization of monomer **7**

Table 3
Electrochemical characteristics of **6** and **7**.

| Compound | E_{ox} (V) | HOMO ^a (eV) | E_g^{optb} (eV) | LUMO ^c (eV) |
|----------|--------------|------------------------|-------------------|------------------------|
| 6 | 0.11 | −4.91 | 2.98 | −1.93 |
| 7 | 0.17 | −4.97 | 2.86 | −2.11 |

^a HOMO = 4.8 + E_{ox} .

^b Obtained from UV spectra $E_g^{opt} = 1240/\lambda_{onset}$.

^c LUMO = HOMO − E_g^{opt} .

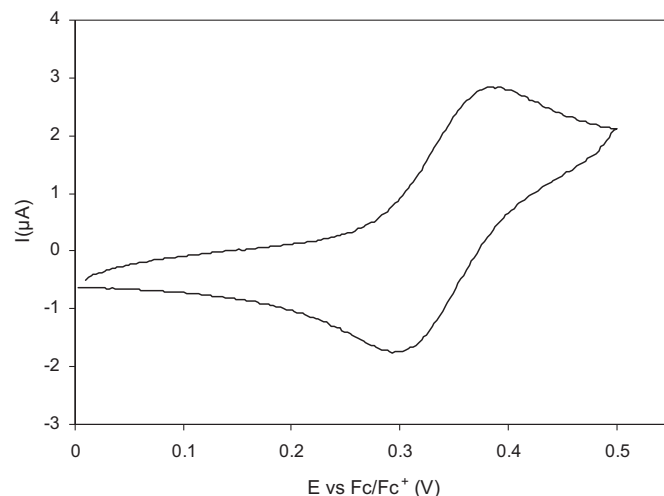


Fig. 7. Cyclic voltammogram of **6** at a scan rate of 50 mVs^{−1}.

containing three reactive vinyl groups started at the lower temperature. Only one exothermic polymerization signal with the maximum at 167 °C was observed for this monomer apparently due to the higher propagation rate. Unfortunately we were not able to fix the glass transition temperature of the product of polymerization of **7**, apparently due to insufficient sensibility of the apparatus used.

The IR spectroscopy was used to examine the extent self-polymerization. The characteristic stretches of vinyl groups of monomers **6** and **7** are found at around 1630 cm^{−1}, 990 cm^{−1} and 908 cm^{−1} [28,29]. After self-polymerization initiated by heating, stretch of vinyl group in the higher frequencies disappear (Fig. 6). The stretches in the fingerprint region disappear or considerably decrease.

The electrochemical data of compounds **6**, **7** are presented in Table 3. The cyclic voltammogram of **6** is shown in Fig. 7. The same values of anodic and cathodic peaks were observed for five times repeated cycles. During the oxidative scan, an anodic peak was observed which can be attributed to the formation of cation radical. The reverse scan showed a reduction process indicating a good electrochemically stability. The oxidation potentials were calculated as the average of the anodic and cathodic peak potentials. The easier oxidation of **6** compared to **7** can be explained as due to the presence of electron-rich methoxy groups. The HOMO energy levels established from the oxidation potentials are comparable (−4.91 eV and −4.97 eV). The LUMO energy levels were calculated from HOMO and optical band gap values. Compound **7** showed lower LUMO energy level (−2.11 eV) than compound **6** (−1.93 eV).

The photoelectrical characteristics of compounds **6**, **7** are summarized in Table 4. The ionization potentials (I_p) values of the amorphous films of monomers **6** and **7** were found to be comparable (5.22 and 5.29 eV).

Charge-transporting properties of the layers of compounds **6**, **7** prepared by spin coating were estimated by XTOF technique. The electric field dependencies of hole-drift mobilities of the layers of **6**,

Table 4
Photoelectrical characteristics of **6** and **7**.

| Compound | I_p (eV) | μ_0^a (cm ² /Vs) | μ^b (cm ² /Vs) |
|----------|------------|---------------------------------|-------------------------------|
| 6 | 5.22 | 2.8×10^{-5} | 2.2×10^{-3} |
| 7 | 5.29 | 9×10^{-5} | 3.5×10^{-3} |

^a Zero field mobility.

^b At an electric field of 6.4×10^5 cm²/V.

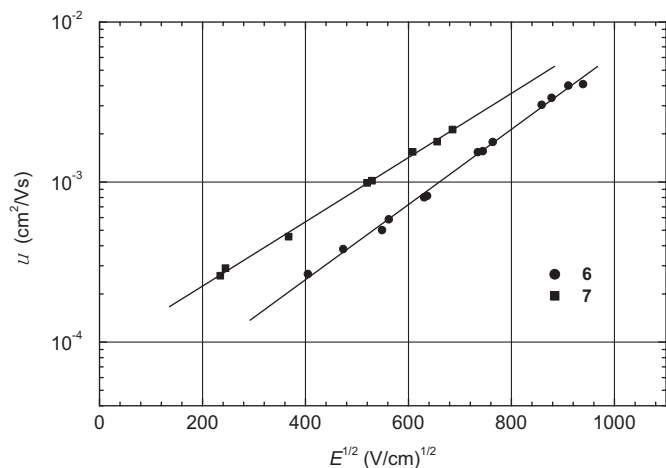


Fig. 8. Electric field dependencies of hole-drift mobilities in the layers of hydrazones **6** and **7**.

7 are presented in Fig. 8. Compound **7** having three hydrazone moieties exhibited better charge-transporting properties. Hole-drift mobility in the layer of **7** reached $3.5 \times 10^{-3} \text{ cm}^2/\text{V}$ at an electric field of $6.4 \times 10^5 \text{ cm}^2/\text{V}$.

4. Conclusions

Two triphenylamine-based hydrazones with reactive vinyl groups were synthesized and their properties were studied. The synthesized monomers form glasses with glass transition temperatures ranging from $52 \text{ }^\circ\text{C}$ to $82 \text{ }^\circ\text{C}$. Ionization potentials of hydrazone monomers are comparable and range from 5.22 eV to 5.29 eV as determined by electron photoemission method. Time-of-flight hole-drift mobility of hydrazone monomer having three hydrazone moieties with vinyl groups is $3.5 \times 10^{-3} \text{ cm}^2/\text{V}$ at an electric field of $6.4 \times 10^5 \text{ cm}^2/\text{V}$. The possibility of self-polymerization of the synthesized monomers was demonstrated by differential scanning calorimetry. Self-polymerization of compound having three hydrazone moieties starts at lower temperature than of hydrazone with one reactive functional group.

Acknowledgments

Financial support of this research by the Research Council of Lithuania (project No. MIP-64/2010) is gratefully acknowledged. Dr. habil. Valentas Gaidelis is thanked for the help in the measurements of ionization potentials.

References

[1] Pron A, Gawrys P, Zagorska M, Djurado D, Demadrille R. Electroactive materials for organic electronics: preparation strategies, structural aspects and characterization techniques. *Chem Soc Rev* 2010;39:2577–632.
 [2] Weiss DS, Abkowitz M. Advances in organic photoconductor technology. *Chem Rev* 2010;110:479–526.

[3] Hains AW, Liang Z, Woodhouse MA, Gregg B. Molecular semiconductors in organic photovoltaic cells. *Chem Rev* 2010;110:6689–735.
 [4] Ripaud E, Mallet C, Allain M, Leriche P, Frere P, Roncali J. Extended triphenylamine conjugated systems derivatized by perfluorophenyl groups. *Tetra Lett* 2011;52:6573–7.
 [5] Bricaud Q, Cravino A, Leriche P, Rancoli J. Poly(thiophenes) derivatized with oligo(oxyethylene) chains as donor materials for organic solar cells. *Sol Energy Mater Sol Cells* 2009;93:1624–9.
 [6] Lygaitis R, Getautis V, Grazulevicius JV. Hole-transporting hydrazones. *Chem Soc Rev* 2008;37:770–88.
 [7] Borsenberger PM, Weiss DS. Organic photoreceptors for xerography. New York: Dekker; 1998.
 [8] Aich R, Tran-Van F, Goubard F, Beauch L, Michaleviciute A, Grazulevicius JV, et al. Hydrazone based molecular glasses for solid-state dye-sensitized solar cells. *Thin Solid Films* 2008;516:7260–5.
 [9] Lav TX, Tran-Van F, Vidal F, Peralta S, Chevrot C, Teysie D, et al. *Thin Solid Films* 2008;516:7223–9.
 [10] Leng B, Tian H. A unimolecular half-subtractor based on effective photoinduced electron transfer and intramolecular charge transfer processes of 1,8-naphthalimide derivative. *Austr J Chem* 2010;63:169–72.
 [11] Li H, Li N, Sun R, Gu H, Ge J, Lu J, et al. Dynamic random access memory devices based on functionalized copolymers with pendant hydrazone naphthalimide group. *J Phys Chem C* 2011;115:8288–94.
 [12] Mitschke U, Bauerle P. Electroluminescence of organic materials. *J Mater Chem* 2000;10:1471–507.
 [13] Muller CD, Falcou A, Reckefuss N, Rohahn M, Wiederhirn V, Rudati P, et al. Multi-colour organic light-emitting displays by solution processing. *Nature* 2003;421:829–33.
 [14] Nuyken O, Jungermann S, Wiederhirn V, Bacher E, Meerholz K. Modern trends in organic light-emitting devices (OLEDs). *Monats Chem* 2006;137:811–24.
 [15] Huang F, Cheng YJ, Zhang Y, Liu MS, Jen AKY. Crosslinkable hole-transporting materials for solution processed polymer light-emitting diodes. *J Mater Chem* 2008;18:4495–509.
 [16] Getautis V, Grazulevicius JV, Malinauskas T, Jankauskas V, Tokarski Z, Jubran N. Novel families of hole-transporting monomers and polymers. *Chem Lett* 2004;33:1336–7.
 [17] Getautis V, Grazulevicius JV, Daskeviciene M, Malinauskas T, Jankunaite D, Gaidelis V, et al. Novel hydrazone based polymers as hole transporting materials. *Polymer* 2005;46:7918–22.
 [18] Getautis V, Grazulevicius JV, Daskeviciene M, Malinauskas T, Gaidelis V, Jankauskas V, et al. Novel hydrazone moieties containing polymers for optoelectronics. *J Photochem Photobiol A Chem* 2006;180:23–7.
 [19] Ostrauskaite J, Voska V, Buika G, Gaidelis V, Jankauskas V, Janeczek H, et al. Novel hole-transporting hydrazones. *Synth Met* 2003;138:457–61.
 [20] Miyamoto E, Yamaguchi Y, Yokoyama M. Ionization potential of organic pigment film by atmospheric photoelectron emission analysis. *Electrophotochemistry* 1989;28:364–70.
 [21] Montrimas E, Gaidelis V, Pazera A. Kinetics of photodischarge of negatively charged layers of Se. *Lith J Phys* 1966;6:569–73.
 [22] Vajiravelu S, Lygaitis R, Grazulevicius JV, Gaidelis V, Jankauskas V, Valiyaveetil S. Effect of substituents on the electron transport properties of bay substituted perylene diimide derivatives. *J Mater Chem* 2009;19:4268–75.
 [23] Mimaite V, Ostrauskaite J, Gudeika D, Grazulevicius JV, Jankauskas V. structure-properties relationship of hydrazones containing methoxy-substituted triphenylamino groups. *Synth Met* 2011;161:1575–81.
 [24] Mallegol T, Gmouh S, Mesiane MAA, Blanchard-Desce M, Mongin O. Practical and efficient synthesis of tris(4-formylphenyl)amine, a key building block in materials chemistry. *Synthesis* 2005;11:1771–4.
 [25] Ostrauskaite J, Voska V, Antulis J, Gaidelis V, Jankauskas V, Grazulevicius JV. High hole mobilities in carbazole-based glass-forming hydrazones. *J Mater Chem* 2002;12:3469–74.
 [26] Chen CC, Duh YS, Shu CM. Thermal polymerization of uninhibited styrene investigated by using microcalorimetry. *J Hazard Mater* 2009;163:1385–90.
 [27] Huang F, Cheng YJ, Zahang Y, Liu MS, Jen AKY. Crosslinkable hole-transporting materials for solution processed polymer light-emitting diodes. *J Mat Chem* 2008;18:4495–509.
 [28] Liao YH, Rao MM, Li WS, Yang LT, Zhu BK, Xu R, et al. Fumed silica-doped poly(butyl methacrylate-styrene)-based gel polymer electrolyte for lithium ion battery. *J Membr Sci* 2010;352:95–9.
 [29] Lizotte JR, Long TE. Stable free-radical polymerization of styrene in combination with 2-vinylnaphthalene initiation. *Macromol Chem Phys* 2003;204:570–6.